Sensors & Diagnostics

TUTORIAL REVIEW

View Article Online
View Journal | View Issue

Cite this: *Sens. Diagn.*, 2024, **3**, 165

Conductive polymer nanocomposites: recent advances in the construction of electrochemical biosensors

Hui Zeng,†[a] Ying Xie,†[a] Tao Liu,[a] Zhenyu Chu,[a] Eithne Dempsey *[b] and Wanqin Jin *[a]

Accompanying the fast development of clinical medicine and materials science, electrochemical biosensors continue to play a significant role in relation to disease diagnosis due to their short time to result, sensitivity and low cost. Since the 2000 Nobel Prize was awarded to conductive polymers (CPs), CP nanocomposites (CPNs) have gradually gained attention in the construction of electrochemical biosensors. Particularly in the last decade, the research hotspot shifted to the precise nanostructure control of CPNs in order to obtain regular geometric shapes enabling improved analytical performance of fabricated biosensors. In this review, we mainly focus on recent progress of regular-nanostructured CPNs used to construct advanced electrochemical biosensors. Emphasis will be placed on the nanostructure control approaches in relation to CPNs comprised of various CPs and their doping materials including metal, metal oxide, carbon materials and coordination compounds. Moreover, we carefully discuss the advantages and disadvantages of these CPNs and their impact on performance according to the various transduction and recognition principles of electrochemical biosensors, such as enzyme electrodes, apta and immunosensors. Finally, we look ahead to the main challenges and prospective research directions for CPNs based electrochemical biosensors.

Received 24th June 2023,
Accepted 27th November 2023

DOI: 10.1039/d3sd00160a

rsc.li/sensors

1. Introduction

Identification and determination of specific physiological components (biomarkers, IgGs, DNA, metabolites *etc.*) in biological samples including blood, serum and body fluids play an essential role in the diagnosis of diseases and guidance of clinical treatments. With the rapid development of clinical medicine, more and more biological targets are being verified to directly correspond to specific diseases or

[a] *State Key Laboratory of Materials-Oriented Chemical Engineering, College of Chemical Engineering, Nanjing Tech University, Nanjing 211816, P. R. China. E-mail: wqjin@njtech.edu.cn*
[b] *Department of Chemistry, Kathleen Lonsdale Institute for Human Health, Maynooth University, Maynooth Co., Kildare, Ireland. E-mail: eithne.dempsey@mu.ie*
† The authors contribute equally to this work.

Hui Zeng

Hui Zeng received his BEng degree from Nanjing Tech University in 2017 and MEng degree in chemical engineering and technology from Nanjing Tech University in 2021 under the supervision of Prof. Wanqin Jin and Prof. Zhenyu Chu.

Ying Xie

Dr. Ying Xie is an associate professor in Chemistry and Molecular Engineering at Nanjing Tech University. She received her PhD degree from Institute of Chemistry, Chinese Academy of Sciences in 2014. She undertook a post-doctoral position at Nanjing Tech University during 2018–2022. Her research mainly focuses on electrochemical biosensors based on regular-nanostructure materials.

physiological state, such as glucose to diabetes,[1–4] troponin to myocardial infarction,[5–8] alpha fetoprotein to liver cancer,[9–11] prostate specific antigen to prostate cancer,[12] human mucin-1 to breast cancer,[13] amyloid-beta to Alzheimer's disease,[14] SARS-CoV-2 spike protein to COVID 19 disease.[15–17] Therefore, the accurate and fast detection of such small molecules or macromolecules justifies the keen interest shown by interdisciplinary researchers in the fields of biochemistry, chemistry, immunology, clinical medicine, engineering and materials science. The biochemistry and ELISA technology which is fundamental to commercial clinical analysers in hospitals or test centres can guide electrochemical biosensor development, taking advantage of home testing for rapid point of site analysis, also benefiting emergency centres.

Since Clark and Lyons created the first electrochemical glucose biosensor in 1962,[18] three generations of electrochemical biosensors have been proposed according to different signal transfer approaches.[19,20] Much attention has been placed on electrochemical biosensors, being driven by the concurrent design and fabrication of novel nanomaterials with associated benefits. Such nanoscale materials display interesting electrical and catalytic properties which are exploited in biosensing performance.[21–23] Within such materials, nanostructured conductive polymers have emerged as interesting contributors to this field.[24,25]

Tao Liu

Dr. Tao Liu received his B.Sc. degree in chemical engineering from the Department of Chemical Engineering, Nanjing Tech University, China in 2017. Currently he is undertaking the post-doctor research at Nanjing Tech University. His current research mainly focuses on the design and synthesis of advanced biosensing materials and the development of electrochemical biosensors.

Zhenyu Chu

Dr. Zhenyu Chu is a professor of chemical engineering at Nanjing Tech University. He received Ph.D degree from Nanjing Tech University in 2013. He studied in Institute of Technology Tallaght, Dublin, Ireland as a collaborative visitor in 2011. He worked as a visiting professor in Curtin University, Australia from 2017 to 2018. He serves as member of Anesthesiology Committee of China Research Hospital and Medical, Biological Membrane Committee in Chinese Industry Association. His research is mainly focused on the design and preparation of novel nanomaterials based electrochemical biosensors for the performance enhancement.

Eithne Dempsey

Dr. Eithne Dempsey received a PhD in Electroanalytical Chemistry from Dublin City University followed by postdoctoral research at St. Vincent's Hospital, Dublin. She then took up a position as Lecturer in Chemistry at Technological University Dublin – Tallaght Campus. She was appointed visiting Professor of Chemistry at the University of the Western Cape, Capetown, South Africa in 2012 and recently (2017) took up a position at Maynooth University, currently as Associate Professor (since 2020) in Dept. Chemistry. Her core research objective is to address electroanalytical challenges using bespoke (nano)materials integrated with biosensing systems suitable for onsite deployment in multiple application scenarios.

Wanqin Jin

Dr. Wanqin Jin is a professor of Chemical Engineering at Nanjing Tech University, the Director of the State Key Laboratory of Materials-oriented Chemical Engineering. He received his Ph.D. from the Nanjing University of Technology in 1999. He was a research associate at the Institute of Materials Research & Engineering of Singapore (2001), an Alexander von Humboldt Research Fellow (2001–2013), visiting professors at Arizona State University (2007) and Hiroshima University (2011). His research focuses on nanomaterials-based electrochemical biosensors. He has published over 300 papers, 4 monographs, and held 65 patents. He is now an editor of Journal of Membrane Science.

While the majority of organic polymers tend to be insulating, conductive polymers hold conductivity between that of a semiconductor and a metal as a result of their π electron (delocalised) system with alternating single and double bonds in the main chain which generally includes heteroatoms such as N and S. The conjugation allows electrons to flow freely along the chain pathway, resulting in conductivity over the range of 10 to 10 000 S cm^{-2}. This is achieved with the help of dopants, which produce "holes" along the length of the polymer chain as charge carriers, showing different electronic conductivity due to different band gaps and Eg values.[26] The earliest report on CPs was delivered by a Japanese scientist, Hideki Shirakawa, who first synthesized polyacetylene. When the *trans* structure accounts for 20%, the conductivity of polyacetylene is 2.35 × 10^{-6} S cm^{-1}.[27] Alan G. MacDiarmid and Alan J. Heeger later published their extensive research on polysulfide nitride. These three scientists shared the Nobel Prize in chemistry in 2000 for their work.[28] Since then, this family of materials continues to attract more and more interest and the number of published peer reviewed scientific articles has increased year on year with more than 500 articles as an annual average, and the number of related patents has also increased with a European Patent Office search (**https://espacenet.com**) returning >10 000 results and the USA (**https://uspto.gov/patents/search**) returning 140 664.

Among various CPs, polyacetylene, poly(3,4-ethylenedioxythiophene) (PEDOT), polythiophene, polystyrene (PS), polypyrrole (PPy) and polyaniline (PANI) are the most studied[29] because of their good stability, ease of preparation and low cost. Recently, some new CPs and CP complexes have emerged, such as poly(benzodifurandione) (PBFDO) with ultrahigh conductivity,[30] PEDOT:$CF_3SO_{2(x)}PSS_{(1-x)}$ with electrochemical stability and air stability,[31] poly(EDOT-thioacetate-*co*-EDOT) with the possibility of forming reversible disulfide bonds.[32] Usually, the performance of CPs is affected by the surrounding medium such as pH, electrolyte, the presence of oxygen and therefore the matrix and operating conditions influence their practical deployment. Besides, compared with other widely applied materials including noble metals, metal oxides and coordination compounds, CPs do not act to magnify the biosensing signal. Meanwhile, their poor solubility and distribution greatly affects the morphology during film formation in biosensor preparation, which causes local aggregation with an increase in film resistance. In order to solve these limitations, metal nanomaterials can be added to form structured composites. The synergy of the two materials is effectively utilized, which greatly improves the conductivity of the composites and shortens the detection time. However, this strategy relied on the dispersion and morphology of different materials in the prepared composite film. Hence, many researchers have addressed precise nanostructure control of the CP nanocomposite (CPN) film in the past ten years. However, there are few reviews which have focused on the area of biosensing coupled with nanocomposites of CPs.

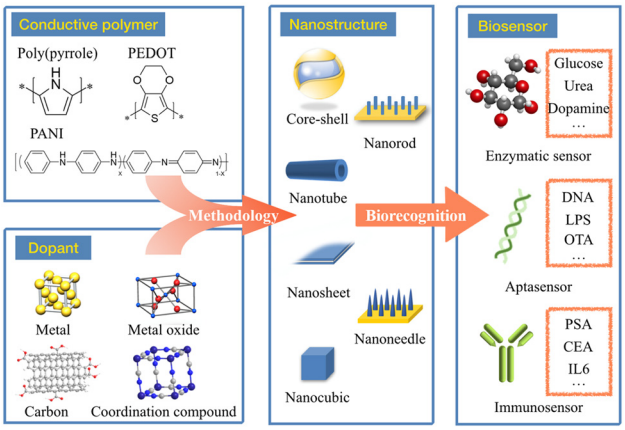

Fig. 1 Schematic of electrochemical biosensors based on CPNs.

In this review, we mainly focus on nanostructured CPNs for the construction of advanced electrochemical biosensors (Fig. 1). The routine synthetic methods for pure CPs and their applications are mentioned in order to present a brief introduction to those traditional materials. Emphasis will be placed on novel CPNs and the various nanostructure control approaches which exhibit regular morphologies. The advantages and disadvantages of these nanostructured composites will be carefully discussed to evaluate their different characteristics in providing a reference for material selection. Finally, the performance of these CPNs based electrochemical biosensors will be compared according to different analytes, indicating the general improvement of sensing ability due to the formation of regular nanostructures. It is expected that this review will guide researchers in the design and nanostructured control of novel CPNs, as well as giving inspiration to construct advanced high-performance biosensors.

2. Traditional preparation methods and biosensing characteristics of CPs

2.1 Traditional preparation methods

In earlier research, CPs were prepared as electrode modifiers for biosensors owing to their conductivity and capability for biomolecule entrapment relative to traditional polymers. Generally, most CPs can be prepared *in situ* on electrode surfaces using traditional methods, including chemical polymerization and electropolymerization. Chemical polymerization is a conventional method of monomer polymerization using active substances such as ammonium persulfate, ferric ions, permanganate or bichromate anions, or hydrogen peroxide.[29] Chemical polymerization usually produces nanomaterials in powdered form with scale-up possibility. However, this method shows limited control in relation to nanostructures. The electropolymerization method involves initial oxidation which results in a radical cation to form a dimer propagating to achieve a polymeric chain.[33] The latter electropolymerization approach is characterized by

its high production efficiency, and during synthesis the polymerization reaction can be controlled by adjusting electrochemical parameters, resulting in controllable morphology.[34,35] Nevertheless, this route is challenging in large-scale production due to the limits of electric power supply and high energy loss.

Since 2000, more and more novel synthesis methods have been continuously developed to precisely control the nanostructure of various CPs in order to obtain regular morphologies, such as the hard template method,[36,37] soft template method,[38,39] electrostatic spinning,[40,41] 3D printing,[42,43] *etc.* The hard template method usually uses a template which acts as a mask to guide the CP growth on the surface or in the channel, so that the obtained nanostructure matches the shape and size of the template. In 2012, Lin *et al.* prepared a vertically oriented PPy nanowire array using a modified ZnO nanowire array as a template.[44] In 2017, Pruna *et al.* adopted a simple two-step electrochemical method by using oriented ZnO crystals as the growth template.[45] In this work, firstly, ZnO nanorods were electrodeposited from $Zn(NO_3)_2$ solution to serve as the skeleton for the PPy formation. Then, the hybridized shells of PPy and graphene oxide (GO) were coated on the core of the prepared nanoarray by electropolymerization, producing a core–shell nanorod feature. Compared with the hard template, the soft template is more readily removed with no damage to the CP morphology. It is mainly used to synthesize CPs with regular morphology by adding specific surfactants and structure-directed molecules. Using polyvinyl alcohol and dodecylbenzene sulfonic acid (DBSA) as structure-directed molecule, He *et al.* synthesized linear PPy and coralline PPy.[46]

Additionally, electrospinning refers to the process that the polymer at the tip of the conductor is rapidly sprayed to the other end of the electrode under the action of high-voltage electric field to form ultrafine nanofibers. Kumar *et al.* prepared PEDOT:PSS/PVA nanofibers using this method in 2016.[47] The prepared nanowires possessed a uniform thickness with diameters of 100 to 200 nm. Within the past five years, 3D printing has become one of the most popular manufacturing techniques to allow rapid and direct preparation of 3D models following digital design.[48] 3D printing has been widely used in the manufacture of biosensor platform due to its customization and precise structure control. Yuk *et al.* introduced a 3D printing strategy using PEDOT:PSS as a raw material to prepare microstructures with high resolution and high aspect ratio.[49] Although the research is still in its early stages, 3D printing has huge potential to be applied in the large-scale biosensor fabrication with a high reproducibility.

In addition to the above methods, new preparation methods have also emerged recently. In 2023, using a new solution-based self-assembly method, Wei *et al.*, successfully prepared a series of 2D-ordered mesoporous CPs and their hybrids under mild conditions, which exhibiting enhanced electrochemical properties. Moreover, the pore size and thickness of obtained nanosheets could be adjusted by changing the chain length of sacrificial templates.[50]

The pure CPs mentioned above have been used to construct various biosensors for detection of different analytes. However, according to the test results of these biosensors, the response time is relatively long due to the slow penetration of the target molecule into the CPs film attributed to high hydrophobicity. Moreover, because of the weak catalysis, pure CPs may not always generate sufficient redox activity to realise the target analysis. The advantages and disadvantages of pure CPs for biosensing applications will be further discussed together with their main characteristics in the following section.

2.2 Characteristics of CPs in biosensing

Among the various applications of CPs, Foulds and Lowe first prepared a PPy film as a biosensing material for the detection of glucose.[51] Since then, many kinds of CPs have been adopted to fabricate various biosensors,[52–55] and the main effects of CPs on the biological recognition and signal response can be generally concluded as detailed below:

First, as a conductive coating, CPs have good environmental stability and can effectively increase corrosion current and voltage, so as to protect internal structure and enhance long-term stability. Second, its excellent conductivity helps to assist charge transfer, so as to improve the electrical properties of electrode materials.[56] This characteristic can allow for rapid response during an enzymatic reaction. In addition, porous structures can be formed with high specific surface area serving as an effective carrier to further load more biological proteins (such as enzymes, antibodies, *etc.*) *via* covalent or other interactions, allowing for more catalytic or binding sites for the detection target. Furthermore, owing to the abundance of functional groups, polymer surfaces are easily modified so as to increase the stability between biomolecules and the electrode surface. For example, the epoxy group of poly(*N*-glycidylpyrrole-*co*-pyrrole) is often used for the immobilization of enzyme molecules. By immersing the modified electrode in galactose oxidase in buffer, galactose oxidase can be covalently connected *via* a functional epoxy group and covalently attached on the surface of the modified electrode.[57] Using this method, the stability of the biosensor can be improved for repetitive detection. Last but not least, the CPs are generally composed of inert molecules, thus they have low toxicity with respect to protein and cell interactions with excellent biocompatibility for *in situ* detection in practical scenarios.

Although the above advantages of CPs are beneficial for the improvement of the biosensing performance including conductivity and protein immobilization, there are still some deficiencies such as weak catalytic activity, which constrain sensitivity and accuracy in relation to analytical performance. Furthermore, in the practical electrochemical process, it has found that with the extension of the long chain, the better the conductivity, the lower the stability.

Owing to these unsatisfactory features, in the last decade, assistance from other functional materials has become

popular in order to construct superior biosensors. Meanwhile, more attention has been paid to the nanostructure control of these nanocomposites *via* development of novel synthesis methods to obtain regular and uniform shapes for strengthening the catalysis and stability. In this way, the biosensing performance is being continuously promoted, resulting in an expansion of target analytes/biomarkers for quantitation. The following sections will introduce the typical nanocomposites along with different categories of doping materials into CPs, as well as discussing the novelty with respect to nanostructures and synthesis methods.

3. Conducting polymer nanocomposites and their nanostructures

Materials employed in the construction of biosensors must not only be able to serve as a bridge between bioactive substances and electrodes, but also to accelerate electron transfer and enhance response, being responsible for providing binding sites for DNA or enzyme surface confinement. CPNs combine polymers with other electroactive materials (especially nanomaterials) with the view to improve the performance of the biosensor, exploiting synergistic effects derived from different components of the composite. Metal nanomaterials, carbon materials, metal oxides and coordination compounds are the most commonly used materials. Furthermore, recent studies have revealed that if the composite can be designed to produce regular and reproducible nanostructures, the biosensing performance will be dramatically improved.[58–61] Therefore, the following discussions will focus on the methodology of nanostructure control in CPNs and their constructed nano-shapes.

3.1 Metal-CP nanocomposites

Amongst the metals, gold, silver, copper and platinum are widely used in doping CPs to further improve the catalytic and conductive properties of electrode materials. At present, although it is very easy to reduce the particle size to nanometer scale, the stable and uniform distribution of nanoparticles has always been a challenge. Scientists have designed a number of new strategies to weaken the aggregation behavior during the formation of thin film. For example, using regular CPs as growth substrates to induce the dispersed growth of metal particles is an effective method to ensure regular nanostructures, which greatly increases the specific surface area of biosensors and provides binding sites for more biological components. In addition, metallic materials will also be used as the core to guide the growth of CPs, so as to form composite nanostructures that are difficult to form spontaneously. Therefore, CPs are gradually being applied in combination with metals to form composites with better electrochemical properties.

In the construction of metal-CPNs, nanowired CPs are mostly built to realize the regular crystallization of metals. Nanowires are a kind of one-dimensional structure with a high aspect ratio which can provide abundant growth sites along its long axis for metal ions to achieve a uniform distribution. Zhang *et al.* followed this strategy to design a Cu/PPy nanowired composite for the electrode preparation.[62] They first prepared a PPy nanowires modified electrode by potentiostatic deposition. Then, Cu/PPy nanowires were obtained by repetitive potential scanning. Electrochemical experiments showed that this composite has excellent catalytic activity and conductivity for the detection of H_2O_2. Besides Cu, silver has served as an outerlayer to deposit on PPy nanowires. Ghanbari *et al.* used a double pulse technique to synthesize silver nanoparticles in an aqueous solution containing $AgNO_3$ and $NaNO_3$. In the double pulse method, two constant pulse currents will pass through the electrode in turns, which is often used to modify the electrode surface with a larger real area. By means of this deposition, PPy nanowires were prepared to present about 100 nm diameter with a high distribution density, and the average size of Ag nanoparticles was about 50 nm (Fig. 2a–c). This architecture effectively couples the high catalysis of Ag and conductivity of PPy together. The oriented nanowire structure can greatly shorten the transfer pathway of electrons to decrease the resistance, and nanoparticles can effectively increase the surface area of nanowires to promote adsorption sites and enhanced activity for the biomolecule.[63] Besides PPy nanowires, PEDOT nanowires can also serve as a skeleton for Pt nanoparticles (PtNPs). The PEDOT nanowire was obtained by electropolymerization in an electrolyte solution composed of EDOT and tetrabutylammonium hexafluorophosphate. Then PtNPs were modified on the PEDOT nanowires by cyclic voltammetry scanning in a H_2PtCl_6 and KPF_6 mixed solution. Compared with the bulk electrode, this nanocomposite presented 11 times higher current density.[64]

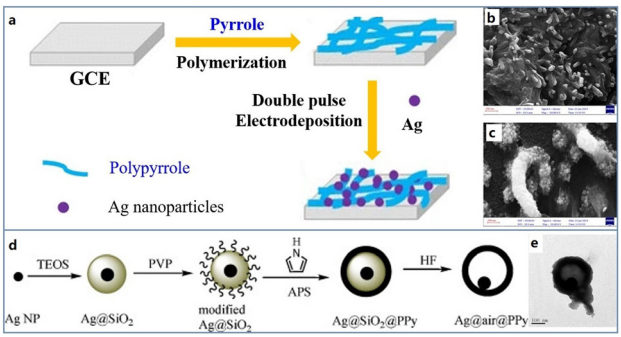

Fig. 2 (a) Schematic diagram of the preparation of Ag/PPy/glassy carbon modified electrode; FESEM images of PPy (b) and Ag/PPy (c). Reproduced from ref. 63 with permission from Elsevier, copyright 2015. (d) Schematic diagram of the synthesis of the yolk–shell Ag@PPy nanoparticles. (e) TEM image of Ag@PPy yolk–shell nanoparticles. Reproduced from ref. 65 with permission from Elsevier, copyright 2010.

In addition to the nanowire structure, many other regular nanostructures have been successfully constructed for these composites. Wang *et al.* designed a yolk–shell nanostructure to integrate Ag and PPy. Ag nanoparticles were first synthesised by a polyol method (Fig. 2d and e), and then ethyl orthosilicateisopropanol solution was dropwise added, resulting in silica coated Ag nanoparticles.[65] Subsequently, poly(vinyl pyrrolidone) (PVP) was employed for encapsulation, and pyrrole monomer solution was introduced for polymerization. Finally, the nanoparticles were immersed in HF aqueous solution to remove the silica layer so that an Ag@PPy yolk–shell nanocomposite was harvested. Although its preparation route is complex and time consuming, this structure is special in a movable silver core, which can be used for encapsulation of enzymes, drugs, *etc.* and nanoreactors for catalytic reactions. A well-defined Pd/PEDOT nanosphere was successfully prepared through a one-step chemical synthesis method. Jiang *et al.* applied EDOT ethanol solution to reduce H_2PdCl_4 solution under a vigorous stirring.[66] In this way, Pd/PEDOT nanospheres with a uniform size of 60 nm were obtained, and Pd nanoparticles possessing 4.5 nm diameter were anchored on the surface of PEDOT. This nanocomposite was applied to recognize H_2O_2 with excellent sensitivity derived from its high electrocatalytic activity and low resistance. In the actual detection, the detection sensitivity reaches 215.3 $\mu A\ mM^{-1}\ cm^{-2}$.

The formation of the two structures above mostly rely on the before formed morphology of CPs to guide the regular growth of metals. On the contrary, the morphology of metal-CPNs can also be controlled by using the regular nanostructure of noble metals. Xiao *et al.* prepared an amperometric biosensor for glucose detection by a nanoporous PEDOT/Au film.[67] The Au film was treated with concentrated nitric acid to obtain a nanoporous structure. Then glucose oxidase was embedded in an ultrathin PEDOT layer of 10 nm during the electrochemical polymerization of EDOT. The morphology of the PEDOT layer followed the nanoporous structure of the Au substrate, benefiting the immobilization of glucose oxidase while improving stability and maintaining activity.

In 2022, Hryniewicz and coworkers prepared AuNPs-modified PPy nanotubes (PPy-NT) in stainless steel mesh electrodes *via* electropolymerization and electrodeposition.[68] The nanotube form of PPy-NT/AuNPs has a better charge transfer process and a higher surface area. When used for COVID-19 impedance detection of SARS-CoV-2 antibodies, the nanotube-based sensor was nearly eight-fold more sensitive than the sensor based on the globular morphology.

Overall, composites of noble metals and CPs are an effective strategy in the construction of biosensing materials, providing not only regular morphologies, but also synergistic effects of excellent conductivity and electrocatalytic activity. However, this type of composites faces some challenges. CPs often lack effectively functional groups to produce strong interactions with metals, leading to poor stability during the electrochemical reaction and low reproducibility for the large-scale fabrication. Besides, most of employed metals are in the ground state, being easily oxidized in air impacting activity. Thereby, difficult storage for maintaining the performance of CPs-metal composites is also a key problem to the wide application for biosensing.

3.2 Metal oxide-CP nanocomposites

Metal oxides can be directly employed in the fabrication of biosensors but may have poor conductivity. Therefore, CPs can serve as the conductivity promoter for metal oxides in the preparation of biosensing materials.

Compared with other materials, metal oxides are easier to form various oriented structures which are often employed as hard templates, such as Al_2O_3, ZnO, TiO_2, NiO, *etc.* Hence, the metal oxide-CPNs enable present many regular features by following the original morphology of metal oxides. Zhu *et al.* used TiO_2 nanotubes as a template to couple with PANI for the detection of glucose (Fig. 3a and b).[69] Firstly, TiO_2 nanoparticles were converted into nanotubes by a hydrothermal method, and then the obtained TiO_2 nanotubes were added into a solution containing aniline and HCl. PANI was wrapped along the nanotubes by oxidative polymerization to generate TiO_2–PANI composite. Authors confirmed that the introduction of PANI covering the TiO_2 nanotubes significantly increased the current signal by 55% with a good sensitivity of 11.4 $\mu A\ mM^{-1}$ during glucose recognition studies. The above growth of PANI relies on the outer surface morphology of TiO_2 nanotubes for shape control. In a different fashion, Yang *et al.* adopted the strategy of nanotube filling to achieve the regular nanostructure of CPs.[70] TiO_2 nanotubes with the tube size of 165 nm were also prepared on the surface of pretreated titanium disc by an anodic oxidation. Subsequently, TiO_2 nanotubes were directly used as working electrodes, and TiO_2–PEDOT nanotube arrays were prepared by potentiostatic deposition. The nanocomposites showed much higher activity than pure TiO_2 nanotubes in electrochemical biosensor and excellent redox reversibility.

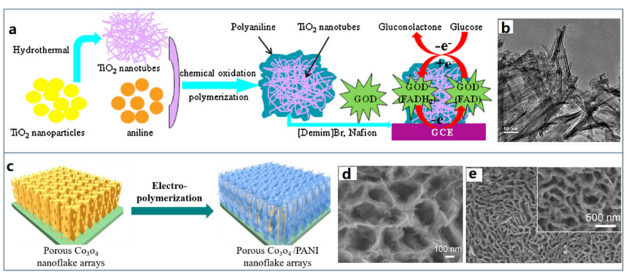

Fig. 3 (a) Schematic diagram of the formation of biosensor based on the nanotubic TiO_2–PANI composite. (b) TEM image of nanotubic TiO_2–PANI composite. Reproduced from ref. 69 with permission from Elsevier, copyright 2015. (c) Schematic diagram of the preparation methods of porous Co_3O_4/PANI nanoflake array. (d and e) SEM image of porous Co_3O_4/PANI nanoflake arrays. Reproduced from ref. 73 with permission from Elsevier, copyright 2017.

Normally in the preparation of TiO_2-CPNs, TiO_2 is always employed as a growth skeleton to control the formation of CPs nanostructure. However, CPs are also capable of providing the crystallization template for metal oxides to produce regular nanostructures. For example, using the electrodeposition method, Py can be induced to orientally polymerize, which *in situ* produces PPy with a nanowire structure on a substrate. In this way, PPy nanowires provide a large surface area for the further deposition of metal oxides. Following this strategy, Meng *et al.* prepared a nanocomposite film of Cu_xO (mixture of CuO and Cu_2O)/PPy nanowires to fabricate a glucose biosensor.[71] PPy nanowires were obtained through potentiostatic deposition, and then Cu nanoparticles were electrodeposited on the surface of nanowires. Finally, the Cu nanoparticles were further oxidised to copper oxide (Cu_xO) nanoparticles by a repetitive cyclic voltammetry, obtaining a Cu_xO/PPy nanocomposite modified electrode. Compared with CuO or Cu_2O modified electrode, Cu_xO modified electrode has a wider linear detection range for glucose detection due to the synergistic oxidation effect of CuO and Cu_2O. At the same time, nanostructured Cu_xO particles can greatly increase the electrocatalytic active region and promote electron transfer due to their well dispersion produced by the PPy nanowires.

In addition to nanowires, scientists have also developed many other three-dimensional nanostructures of metal oxide-CPNs, such as core–shell nanospheres and nanosheets arrays. Yang *et al.* prepared a PPy coated Fe_3O_4 core–shell nanoparticles for the glucose detection.[72] Fe_3O_4 nanoparticles were first prepared by a hydrothermal co-precipitation of Fe^{2+} and Fe^{3+} ions in ammonia solution. In order to create the core–shell structure, the Fe_3O_4 nanoparticles were dispersed in pyrrole phosphate buffer solution for polymerization. According to the electrochemical characterization in a real serum sample, this core–shell nanostructure is not only an ultralarge surface area for the immobilization of glucose oxidase, but also excellent conductivity derived from PPy shell. As a result, the as-prepared biosensor enabled a wide detection range from 0.5 μM to 34 mM, satisfying most requirements in clinical diagnosis of diabetes. Mai *et al.* delivered a kind of oriented Co_3O_4 nanosheets as a template to induce the PANI growth.[73] Firstly, porous Co_3O_4 nanoplate arrays were synthesized by a hydrothermal method. After *in situ* formation of dense Co_3O_4 nanoparticles on a substrate, this film was annealed in Ar atmosphere to obtain the self-supporting porous Co_3O_4 nanoplate arrays. The core–shell structure was achieved by the electropolymerization of PANI to cover the whole surface of nanoplates. Imposing a constant anode current density of 3 mA cm^{-2} for 1800 s, an oriented feature of Co_3O_4/PANI core–shell arrays was observed (Fig. 3c–e). This morphology was mainly derived from the regular three-dimensional structure of Co_3O_4 nanosheets. As a result, the nanostructure shortened the pathway of electron transfer through the bulk film, producing excellent performance in electron/ion transfer both lengthwise and transverse and structural stability.

In 2021, Lalegül-Ülker and Elçin synthesized silica-coated iron oxide/polyaniline (Si-MNPs/PANI) nanocomposites by a chemical oxidative polymerization method.[74] By adjusting the synthesis conditions, composites with different morphologies such as nanotubes (SPNTs) and granules (SGT) can be obtained. Comparing Si-MNPs/PANI with the same content of SI-MNP, it can be found that SPNT has higher magnetization and SPG has about 30 times higher conductivity. The author believes that the difference in conductivity between the two nanocomposites may be due to the following two factors. On the one hand, the tubular PANI may contain non-conductive aniline oligomers; on the other hand, the uniform distribution of SI-MNPS in SPG may be beneficial to electron transport.

Generally, metal oxides are of the good catalytic activity and regular morphology, but poor in the conductivity due to a large band gap. Using CPs to improve this deficiency is a feasible strategy through the construction of nanocomposites. Regular nanostructures derived from CPs or metal oxides contribute to high specific area and electrocatalysis, benefiting the signal magnification of biosensing reactions. Nevertheless, there are rare organic functional groups (such as $–NH_2$, –COOH, –CO–, *etc.*) on metal oxides, hence, it is difficult to establish effective interactions between metal oxides and CPs. As a result, most of these materials are only reported for one-time use, which may be attributed to their weak stability during the electrochemical redox process. A means of strengthening the binding effects for electrochemical stability is always a challenge.

3.3 Carbon-CP nanocomposites

Although CPs are capable of electron transfer with reliance on their conjugated structure, their conductivities are still much weaker than those of metals or carbon materials. For example, at room temperature, the conductivity of PPy is about 10^2 S cm^{-1}, while 2D materials such as graphene, can reach 10^4 S cm^{-1} in the same conditions. Carbon materials, mainly including graphene, carbon nanotubes, carbon nanofibers, carbon nanospheres *etc.*, have attracted huge attention in various research fields. Due to the hybridisation of electronic orbitals (sp, sp^2, sp^3) such materials have a variety of unique properties at the nanoscale. Functional groups can be easily grafted onto the surface to provide binding sites for anchoring CPs with good stability.

Therefore, carbon materials are gradually being adopted as additives to enhance the properties of CP sensing films.

Based on this idea, Xu *et al.* wrapped multi-walled carbon nanotubes (MWCNTs) with PANI to obtain a uniform core–shell nanostructure.[75] First of all, MWCNTs were dispersed in aqueous solution of DBSA by mechanical stirring and ultrasonication. In this way, the aniline group can be connected to the surface of MWCNTs through an amide bond, providing the growth site for the subsequent growth of PANI. Then, aniline was added and sonicated for 2 hours. Finally, ammonium persulfate (APS) aqueous solution was slowly dropped into the reaction system to initiate polymerization. The conductivity (6.23×10^{-1} S cm^{-1}) of the

obtained composite reached at least one order of magnitude higher than that of pure DBSA doped PANI (1.03×10^{-2} S cm^{-1}). The result showed that the addition of MWCNTs remarkably improved the thermal stability of the composite. In addition, due to the natural compatibility of CPs and carbon materials, their combination is uniform and also can play a synergistic effect to maximize the performance of composite materials. Besides, An *et al.* combined carbon nanotubes with PPy to obtain a composite with excellent electrocatalytic performance.[76] Characterization proved that the composite had both long-term stability and excellent electrocatalytic oxygen reduction performance. Moreover, graphene nanoflakes are one of the commonly used materials to increase electrochemical performance. As shown in Fig. 4a–c, Qi *et al.* prepared core–shell hybrid materials by coating PPy nanotubes (PNT) on graphene nanosheets (GNF).[77] During the synthesis, the N–H position of Py unit was acylated with the carboxyl group of GNF, and the GNF/PNT hybrid was covalently attached on the surface of PNT. In addition, the coating amount of GNF can be controlled by adjusting the mass ratio of GNF to PNT. Graphene has good mechanical strength and impermeability, which not only helps to delay the failure caused by volume change, mechanical deformation and degradation of PNT, but also exhibits strong electron transfer ability due to close binding and electrostatic interaction, coupled with regular nanostructures. The equivalent series resistances, calculated from the high-frequency intercept on the real axis, were 5.1 Ω and 3.9 Ω for GNF/PNT (1 : 3) and GNF/PNT (9 : 1) respectively, which were much lower than that of pristine PNT of 17.9 Ω, suggesting a higher conductivity.

In addition to the above core–shell structures, many other nanostructures have also been studied in order to obtain better material properties. Haq *et al.* considered that most of the existing methods rely on the strict chemical treatment of carbon materials, which will lead to serious degradation of the chemical structure and properties of carbon materials.[78] Therefore, they proposed a novel method to directly grow PANI chains from nitrogen doped carbon nanotubes (NCNTs). In this way, aniline was polymerized along the N-doped sites of the carbon nanotube wall to form a seamless hybrid structure. The prepared NCNTs were first put into aniline solution and kept at 2 °C. Then APS was injected into aniline solution dropwise. The composite could be obtained by changing the reaction time to control the polymerization reaction. Due to the strong electrochemical properties of PANI shell and the synergistic effect of high conductivity NCNTs core, NCNTs–PANI composite was expected to be an ideal material for sensor electrode. The voltammogram presented a nearly rectangular shape, which indicated the efficient proton diffusion migration and high capacitance. Besides, Zhou *et al.* reported a novel composite material coated with a layer of ultra-thin spiny PANI nanorods on graphene nanofibers (GN).[79] This three-dimensional structure has the characteristics of large specific surface area and fast oxidation–reduction rate. Characterization confirmed that the synergistic effect of GN network framework and PANI nanorods significantly increased the energy density (54 W h kg^{-1}) and power density (4.9 kW kg^{-1}) of the nanofiber electrode materials. Song *et al.* attempted to synthesize PANI nanocones by an *in situ* polymerization on the surface of graphene (Fig. 4d–f).[80] This nanocomposite exhibited more charge transfer pathways and faster charge transfer speed due to the coupling effect of the layered graphene and the unique conical structure of PANI with high specific surface area. The interfacial charge transfer resistance of pure PANI is about 13.5 Ω in the high frequency region, while that of the composite was less than 3.3 Ω.

In 2021, Sun *et al.*, achieved the preparation of sea urchin-like porous polyaniline (PPANI) *via* chemical synthesis method in saturated solution, and obtained PPANI/MWCNTs retaining the special porous morphology of PPANI *via* a self-assembly method.[81] Due to the strong π–π interaction between PANI and MWCNTs, stable composite materials can be obtained by self-assembly method. With the formation of porous structures, the specific surface area of PANI and PPANI/MWCNTs is significantly increased. Moreover, authors found that PPANI/MWCNTs could improve the electrochemical properties of Co_9S_8. Co_9S_8 doped with PPANI/MWCNTs exhibits lower charge transfer resistance, superior catalytic activity, higher conductivity, and better cycle stability.

In general, because of the natural binding force between carbon materials and CPs, the synergistic effect is much stronger than other nanocomposites especially showing much lower resistance and higher electrochemical stability. However, there are still two major disadvantages derived from the instinctive characters of carbon materials: one is that carbon materials generally need to be modified before use. This process usually involves strict chemical treatment in the mixture of concentrated nitric acid and sulfuric acid, which will greatly reduce the performance of carbon materials; another one is that carbon materials have

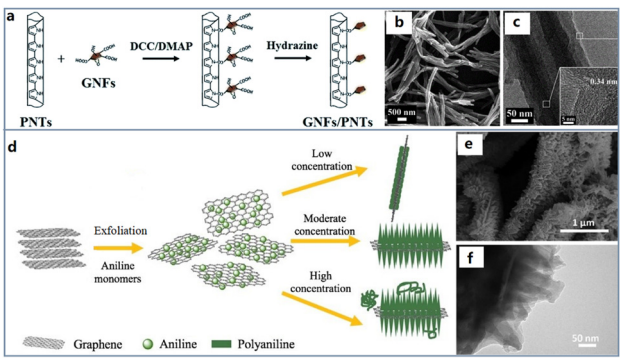

Fig. 4 (a) Schematic diagram of the preparation methods of a core–shell graphene nanosheet coated PPy nanotube. (b) SEM images of pristine PNTs. (c) TEM images of GNFs/PNTs (insets show the corresponding magnified HRTEM images). Reproduced from ref. 77 with permission from Royal Society of Chemistry, copyright 2018. (d) Schematic diagram of the preparation methods of porous PANI/graphene nanocone. SEM (e) and TEM (f) image of graphene/PANI hybrid. Reproduced from ref. 80 with permission from Elsevier, copyright 2018.

insufficient selectivity for target molecules, which greatly limits the detection accuracy in the field of biosensors. Therefore, combining carbon materials with CPs without affecting their original properties is still a main challenge.

3.4 Coordination compound-CP nanocomposites

As per the above discussion, CPs exhibit weak catalytic properties and while the above-mentioned metals and metal oxides can solve this issue for CPs, their high oxidation potentials risk interfering electrochemical signals in practical applications. Therefore, some coordination compounds, such as Prussian blue (PB) and metal organic framework materials (MOFs), are attracting more and more interest as the electrocatalysis unit for incorporation with CPs. PB has been served as a blue pigment since 1906, and then it was confirmed to possess a strong electrocatalytic ability by Itaya.[82] In the unit cell of PB, there are two kinds of iron atoms with different valences of +3 and +2. Therefore, PB enables to play the role of both oxidant and reductant at certain potentials. Normally, it can realize the detection of H_2O_2 which is a common product of enzymatic reactions at only −0.05 V *vs.* Ag/AgCl. In this case, after the immobilization of different enzymes, this material has been applied to fabricate various biosensors for assays of multiple physiological analytes, such as glucose, lactate, glutamate *etc.*[83–87] However, its band gap is about 1.54 eV, hence, the conductivity cannot be satisfactory. In order to overcome this defect, PPy (7.5×10^2 S cm^{-1}), PEDOT (1.0×10^2 S cm^{-1}) and PANI (2.0×10^1 S cm^{-1}) have been widely adopted to connect the crystals as a bridge to accelerate electron transfer and improve the detection performance.

It is worth noting that with the in-depth study of PB, scientists have found that the nanocubic structure of PB crystals enables to provide much larger specific surface area and more active sites derived from its smooth edges for stronger biosensing signals.[88–91] Owing to this result, nanocubic PB was used to form composites with CPs with expected improvement of both catalysis and conductivity. Muthusamy *et al.* first proposed a core–shell PB–PPy nanocubic composite through an *in situ* polymerization method.[92] The authors used a mixed solution containing pyrrole, $FeCl_3$, $K_3[Fe(CN)_6]$ and HCl as the reactant to prepare the nanocomposite. In this reaction, Fe^{3+} played a role of the oxidant to polymerise pyrrole molecules and then it was reduced to Fe^{2+} to coordinate with $[Fe(CN)_6]^{3-}$ for the formation of PB crystals. After stirring for 12 h, a nanocomposite composed of PPy particles covering the PB nanocube was obtained with average size of 100 nm. This nanocomposite was then compared with pure PB to prove its superior conductivity (2 fold increase). In relation to composites of PPy nanoparticles and PB nanocubes, our group developed a nanopore-constrained growth strategy to construct a heterogeneous nanostructure of the PB–PPy nanocomposite on a hollow fiber substrate (Fig. 5a–c).[93] A porous Al_2O_3 hollow fiber is a key to provide a constrained

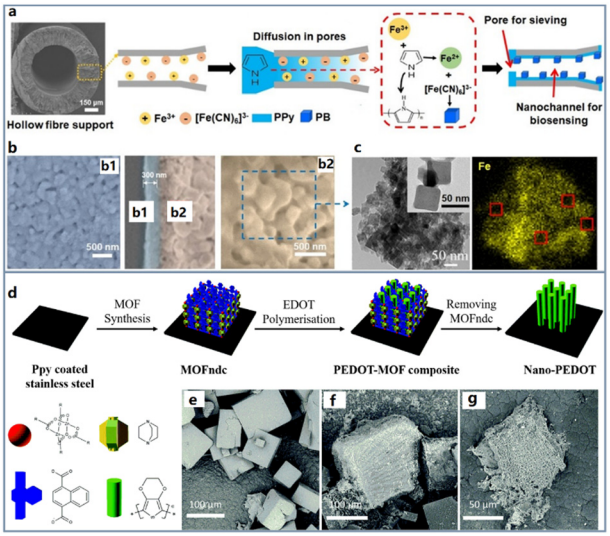

Fig. 5 (a) Schematic diagram of synthesis method combining PPy polymerisation and PB coordination reactions. (b) FESEM images of the separation channel surface (b1) and biosensing channel wall (b2). (c) TEM and mapping images of the surface morphology of the biosensing channel and the distributions of Fe. The red boxes show the selected regions without regular nanocubes. Reproduced from ref. 93 with permission from Wiley, copyright 2020. (d) Schematic diagram of PEDOT growth controlled by MOF uniform pore. SEM images of MOFndc (e), PEDOT-MOF composite (f) and nano-PEDOT (g). Reproduced from ref. 97 with permission from Royal Society of Chemistry, copyright 2017.

space through its numerous nanopores. In order to drive the synthesis into pores, the reactants Fe^{3+} and $[Fe(CN)_6]^{3-}$ firstly filled the pores of hollow fiber by a vacuum force, and then this hollow fiber was immersed into the pyrrole solution for the simultaneous generation of PPy and PB. Due to the structural differences between fiber surface and inner pores, the PPy–PB nanocomposites formed two kinds of morphologies, presenting a surface nanoporous layer and a nanocubes composed nanochannel to achieve serum extraction from whole blood and biosensing of vital physiological indices, respectively. This work indicates that the nanostructure control of CPs based nanocomposites can give not only performance improvement, but also extra functionality for biosensing.

In 2023, Lee and Hong fabricated PB–polydopamine (PDA)–PPY in one step,[94] which was achieved by reducing Fe^{3+} using dopamine (DA) and Py as reducing agents and synthesizing PB nanocubes while copolymerizing. Using two monomers in the synthesis process of composite materials results in better conductivity and stability than using a single monomer. This may be because the addition of DA makes the structure of the copolymer more stable, which is also proved by the easy dissolution of PPy–PB during the electrochemical characterization process.

As defined by Kitagawa,[95] PB is the simplest material in the family of metal organic frameworks (MOFs). By changing –CN– group in PB to other ligands, the cell structure and properties will be greatly different. Initially, MOFs are famous

for the ultralarge surface area from their cell cavities enabling adsorption of huge amounts of small gas molecules, such as CO_2, CH_4, *etc.* Uemura first confirmed that Py was also able to enter into the cell cavity of coordination nanochannels.[96] Since then, Wang *et al.* followed the principle above to further realize the polymerization of the EDOT located in the MOF cavity for the exact control of PEDOT nanostructures, obtaining a vertical nanorod shape (Fig. 5d–g).[97] In this work, PPy coated stainless steel foil was placed into a precursor solution containing $Zn(NO_3)_2{\cdot}6H_2O$ and NDC (naphthalenedicarboxylate), 1,4-diazabicyclo[2.2.2] octane and *N*,*N*-dimethylformamide to prepare the MOF–NDC *in situ* as a growth template for PEDOT. Subsequently, the foil was immersed into a pure EDOT solution for 4 h to allow the monomer molecules to diffuse into the MOF cavity. Due to the space limitation in the cavity, the growth of PEDOT preferred the vertical direction to exhibit a nanorod morphology. This part of PEDOT not only maintained the regular morphology, but also effectively improved the conductivity of the composite. As shown in the volt-ampere curves, the current strength of the MOF–PEDOT composite was at least one order of magnitude higher than that of MOF–NDC (insulator) when the applied voltage is higher than +2 V or lower than −2 V.

The above work focused on inducing the synthesis of composites with regular morphology through the internal pore structure of MOF materials. However, due to the instability of MOF materials, the prepared composites will be more vulnerable, which is a main defect for large-scale production and usage. Therefore, some scientists have paid attention to the external growth of CPs to cover or fix MOFs in their matrix in order to avoid the structural damage during the electrochemical sensing. Xie *et al.* proposed a PPy@ZIF-8/GO aerogels nanocomposite to fabricate an ultrasensitive dichlorophenol biosensor for pollutant detection in a real lake.[98] The authors constructed a porous 3D architecture to lock the ZIF-8 nanocubes in an interconnected network of PPy/GO *via* a two-step synthesis route. Initially, a basic 3D skeleton was built *via* a polymerization reaction of Py enclosed by graphene nanosheets. $FeCl_3$ served as an oxidant to produce PPy/GO which was then treated through a hydrothermal process to form an aerogel structure. Then, this nanocomposite enabled abundant binding sites derived from –NH– group in the PPy chain to attract Zn^{2+} for the crystallization of ZIF-8. In this way, the growth behavior of ZIF-8 has been constrained to form a regular polygonal shape with the size of 150 nm. Compared with the only ZIF-8 modified electrode, this nanocomposite based electrode can evidently decrease the electron transfer resistance from 798.5 to 77.7 Ω, showing a high conductivity attributed to the coverage of PPy. The as-prepared electrode was applied to detect Dcp (2,2-methylenebis (4-chlorophenol)) which is a severe environment pollutant owing to its high toxicity, carcinogenicity and persistence. This sensor exhibited an ultralow limit of detection to 3 nM with a wide linear range from 0.3 nM to 10 μM. If PPy was not adopted to cover ZIF-8, the prepared electrode would show a 10-times higher LOD value. Besides, they have proved that the introduction of PPy can increase the usage stability of the sensor during the repetitive electrochemical detection in the real lake water. This work presents a successful example that CPs are capable to not only reduce the resistance for the electrochemical process, but also enhance the stability through their functional groups which produce certain chemical valences with MOFs. Compared with the synthesis of CPs in the internal pore of MOFs, the external growth of CPs to cover or immobilize MOFs can effectively improve the stability of the composite, and the externally coated CPs provide more active functional groups to facilitate the loading of recognition molecules.

Overall, coordination compounds have relatively poor conductivity and stability to show difficulty for direct applications in the electrochemical biosensing. However, due to their special properties including the polyhedral structure, abundant active sites and large specific surface area, they are capable to serve as a growth template to take advantages of CPs through the intergrowth strategy. Until now, most of coordination compound-CPNs are limited to enzymatic biosensors. The high water resistance and low electron resistance of CPs are effective to improve the electrochemical ability of coordination compounds to strengthen redox process during the enzymatic reaction. Nevertheless, there are still too few coordination compounds available to satisfy the requirement of biosensing materials. With the continuous development of new conductive coordination compounds, this kind of nanocomposite will result in further choices to extend its applications beyond enzymatic biosensing.

4. Applications of nanostructured CPNs in electrochemical biosensors

In Table 1, we listed CPNs-based biosensors used to detect physiological markers. For the detection of physiological markers, enzyme, aptamer and immunological reactions are the main detection principles. These three kinds of biosensors are used to assay different types of physiological indices. The enzymatic biosensor is mainly focused on the detection of small molecules owning their specific enzymatic reactions. The research on glucose analysis dominates almost reported CPNs based enzymatic biosensors. As shown in Table 1, using only PPy as the electrode material to detect glucose is often weak in sensitivity, although its regular nanostructures such as nanotube and nanowire have been successfully synthesized. This result indicates that the nanostructure control of pure CPs may play few effects on promoting the enzymatic reaction due to their instinctive poor catalysis. Therefore, in order to address this issue, metals, metal oxides and carbon materials are preferred to assist CPs for obtaining the sensitivity enhancement.

By using TiO_2 to decorate PPy, the biosensor showed a higher performance of detecting glucose, compared with the

Table 1 CPNs-based biosensors for the detection of physiological markers

	Material	Morphology	Preparation method	Analyte	Detection limit (μM)	Detection range (μM)	Sensitivity (μA mM^{-1} cm^{-2})	Ref.
Enzymatic sensor	PPy	Nanotube	Potentiostatic electropolymerization	Glucose	50	0.2–13 000	12.3	99
	PPy	Nanowire	Electrodeposition	Glucose	100	100–7500	6.12	100
	PPy/TiO_2	Nanotube	Electrodeposition	Glucose	1.5	1.5–600	187.28	101
	PANI	Nanoflower	Chemical synthesis	Glucose	18	1000–30 000	2.03	102
	PANI/AuNPs	Nanosphere	Chemical synthesis	Glucose	10	10–3200	63.1	103
	PANI/PB	Nanoporous	Electrodeposition	Glucose	0.4	2–1600	99.4	104
	PEDOT	Nanoporous	Electrodeposition	Glucose	100	100–10 000	9.24	105
	Fe_3O_4/PPy@ZIF-8	Core–shell	Hydrothermal method	Glucose	0.33	0.001–2	—	106
	SiO_2($LuPc_2$)PANI(PVIA)-CNB	Nanobead	Chemical synthesis	Glucose	100	1–16 000	38.53	107
	PEDOT:PSS @Pt@Pd	Layered structure	Electrodeposition	Glucose	3	10–92 000	247.3	108
	Au-f-MWCNT-PPy	Nanotube	Electropolymerization	Cholesterol	0.1	2–8	10.12	109
Aptasensor	PPy	Nanowire	Chemical synthesis	DNA	1×10^{-7}	1×10^{-7}–0.5	—	110
	PPy–AuNPs	Cauliflower-like	Electrodeposition	DNA	1.50×10^{-8}	1.50×10^{-8}–1	—	111
	PPy/GO-GNP	Nanosheets	Potentiodynamic method	DNA	1×10^{-9}	1×10^{-9}–1	—	112
	PANI	Nanowire	Chemical synthesis	DNA	0.02	0.02–1	—	113
	PANI–PPy–Au	Nanotube	Chemical synthesis Electrodeposition	DNA	1×10^{-7}	1×10^{-7}–1	—	114
	PANI/PEG	Nanowire	Chemical synthesis	DNA	1×10^{-8}	1×10^{-8}–1×10^{-7}	—	115
	PANI–GO	Nanowire	Chemical synthesis	DNA	2.08×10^{-10}	1×10^{-9}–1	—	116
	PEDOT	Sponge like	Electropolymerization	DNA	2×10^{-4}	2×10^{-4}–1×10^{-5}	—	117
	PEDOT–PPy–Ag	Nanotube	Chemical synthesis	DNA	5.4×10^{-9}	1×10^{-8}–1×10^{-5}	—	118
	PEDOT:PSS/RGO	Sponge like	Chemical synthesis	DNA	1.7×10^{-10}	5×10^{-11}–1	—	119
	PPy–Cu-MOF	Nanowire	Chemical synthesis	LPS	0.29 (pg ml^{-1})	1.0–1000 (pg ml^{-1})	—	120
	PEDOT–AuNFs/GOS	Nanoflower	Ionic liquid-assisted one-pot method	OTA	0.0014 (pg ml^{-1})	0.01–20 (pg ml^{-1})	—	121
Immunosensor	PPy–Au NWs	Nanowire	Template method	PSA	0.0003 (pg ml^{-1})	0.01–10 000 (pg ml^{-1})	—	122
	PPyNS/PtHNs@AgPts	Hollow core–shell	Chemical synthesis	PSA	0.1203 (pg ml^{-1})	0.5–50 000 (pg ml^{-1})	—	123
	PPy@HNTs-Pd	Nanotube	*In situ* oxidative polymerization	PSA	0.03 (pg ml^{-1})	0.1–25 000 (pg ml^{-1})	—	124
	PANI@Au@CPS	Nanosphere	Chemical synthesis	CEA	1.56 (pg ml^{-1})	6–12 000 (pg ml^{-1})	—	125
	PANI@MWCNTs/CoS_2	Layer by layer	One step hydrothermal method	CEA	0.33 (pg ml^{-1})	10–40 000 (pg ml^{-1})	—	126
	PPy-NWs	Nanowire	Nano printing	IL6	0.36 (pg ml^{-1})	1–50 (pg ml^{-1})	—	127
	PPyNTs@PtNDs/PDDA/MoS_2	Nanotube	Self-degraded template method	AFP	0.05 (pg ml^{-1})	0.05–50 000 (pg ml^{-1})	—	128
	PANI/graphene	Nanodroplet	Electropolymerization	NGAL	21 100 (pg ml^{-1})	50 000–500 000 (pg ml^{-1})	—	129

Abbreviations: LPS: lipopolysaccharide, OTA: ochratoxin A, PSA: prostate-specific antigen, CEA: carcinoembryonic antigen, AFP: alpha fetoprotein, NGAL: neutrophil gelatinase-associated lipocalin, IL6: interleukin 6.

glucose biosensor which was only using PPy nanowires as the sensing material.[101] Meanwhile, the detection limit was also improved to 1.5 μM reaching more than 30 times higher than that of the PPy nanotube based biosensor. However, its linear range was much lower, which may be attributed to the decreased efficiency of electron transfer when producing more electrons derived from the high sensitivity. Similarly, the glucose biosensor constructed by PANI/AuNPs or PANI/PB nanocomposite also presented a much better performance than the PANI nanoflower based biosensor. Among these, the introduction of PB enabled enhancement of the original sensitivity of PANI to nearly 50 times and decreased the detection limit to 0.4 μM which is only 1/45 of the PANI ability.[104] This is because that PB is well considered as an artificial peroxidase to have outstanding reduction activity for H_2O_2 which is a main product of oxidase reactions. In this way, PB plays a role of signal magnifier in the reaction of glucose oxidase during the glucose detection, promoting the overall performance of PANI. Moreover, if the CP was changed to PEDOT, the employment of noble metals had been also proved to be capable of the enhancement of the biosensing performance. Therefore, the advances of nanocomposites for the enzymatic biosensor are mainly confirmed as the promotion of sensitivity and detection limit.

Aptamer based biosensors are mainly used to detect specific signals by immobilizing aptamer chains (RNA, single stranded DNA or double stranded DNA) for attracting target molecules to produce the response signal. The design of aptasensors largely depend on the different recognition modes which are inherent in each aptamer-target pair given to the electrode surface. Therefore, the sensing material with regular nanostructure is often applied to provide abundant active sites for the uniform and high-density immobilization of the aptamer strand, obviously increasing the probe amount to magnify the detection signal. However, there is normally weak interaction between CPs and aptamers. In this case, the employment of other materials to CPs for the construction of aptasensors is beneficial to enlarge the surface area and denote effective sites for the aptamer loading. For better comparison of the function belonging to the introduced materials for the CPNs, we have listed the performance of several pure CPs (including PPy, PANI and PEDOT) and their nanocomposites prepared aptasensors in Table 1. Noble metals and graphenes are preferred because they form chemical bonds with aptasensors. It can be observed that the nanocomposites generally possessed superior detection limit and linear range than each pure CP. It is interesting that using graphene to integrate with CPs enables superior performance relative to applying noble metals, which is quite different with the enzymatic biosensor. Wang has provided an explanation that graphene is an excellent biocompatible material.[130] There are many functional groups on the surface, which can combine with aptamers more readily. In this case, the carbon material is a preferred supplement to composite CPs in the construction of various aptasensors.

The electrochemical immunosensor relies on the specific binding reaction between antigen and antibody being labelled by certain signal molecule showing the electrochemical redox ability to realize signal transduction. It is rare that immunosensors are reported which employ CPs solely, due to the fact that the immunosensor reaction itself does not produce an electric signal. Therefore, the electrode material is required to supply satisfactory electrocatalysis and conductivity achieving signal magnification, however, CPs are poor in this matter. Thus, materials having both of the above characteristics are encouraging in the preparation of CPs. As shown in Table 1, noble metals, alloy metals, metal sulphides and carbon materials have been prepared to assist PPy and PANI. In relation to cancer biomarkers and cell factors, PSA, CEA, IL6, AFP, NGAL, *etc.*, are reported widely and among these immunosensors, many regular nanostructures of nanocomposites have been created to improve the performance of immunosensors through developing different synthesis methods. Nanowire, nanosphere, hollow core–shell and nanotube can be obtained through the chemical synthesis, *in situ* oxidative polymerization and hydrothermal method. Obviously, the PPy-AuNPs nanowires presented the lowest detection limit to 0.0003 pg ml^{-1} for the recognition of trace PSA considered as the most specific biomarker of prostate cancer, besides, this immunosensor also showed an ultrawide linear range of 0.01–10 000 pg ml^{-1}.[122] The authors claimed that the oriented nanowire structure shortened the path of electron transfer. Moreover, electrostatic interactions between the positively charged AuNPs and the anionic amino acid residues of the antibody results in high binding efficiency to harvest more signal probes. Hence, this sensor is capable of detection of lower concentrations of PSA due to its high response signal.

According to the performance comparison in Table 1, CPNs exhibit a generally better performance than pure CPs in three main categories of electrochemical biosensors. Various regular nanostructures, especially some oriented morphologies, are advanced in their low electron transfer resistances and high electrocatalysis resulting in the high sensitivity, linear range and low detection limit.

5. Conclusion and prospect

We have summarized recent research progress of advanced CPs nanocomposites used to construct various electrochemical biosensors with their classification, preparations and applications. A concept is emphasised that the reasonable design of composites can be used to develop new sensing materials, such as better anti-interference ability, lower detection limit, higher sensitivity, lower sensing temperature and greater stability. Reasonable design requires a more comprehensive understanding of the properties of individual materials and composites. This paper puts forward its own point of view. The metal components in the composites can effectively improve the quantitative capabilities of the sensor, and it is easy to

introduce functional groups coupled with biomolecules, so as to couple to antibody conjugates to detect antigens. It plays an important role in aptamer sensing and immunological (electrochemical ELISA) sensing. The electron exchange process between the conductivity band of metal oxide and adsorbed species is very fast, which can greatly reduce the detection time. Carbon materials can effectively improve the conductivity and chemical stability of the overall composite materials, adapt to more rigorous detection environment, and perform well in detecting metal ions. Due to its special structure, carbon materials also have better detection performance than other materials in protein detection. Coordination compounds can provide better catalytic activity, effectively reduce the detection potential and avoid the influence of interfering substances. They are suitable for complex systems with a variety of interfering substances under detection conditions. In addition, the preparation cost of coordination compounds is generally low, which can reduce the production cost of sensing materials. The introduction of other materials as composites of CP is due to weak catalysis and few active sites for loading biological molecules or proteins. In order to achieve the regular nanostructure of CPs nanocomposites, the control of the original morphology of CPs is a key step and most concerned to provide a skeleton for the further doping other materials to keep their regular growth. According to the performance comparison, the major superiorities of these regular-nanostructured nanocomposites are the abundant catalytic sites and short pathway to accelerate electron transfer rates, together with the adjustable functional groups and charge to match the different proteins and aptamers. Therefore, the integration of CPs and other assisting materials enables strengthening of not only the signal production but also the signal magnification, harvesting a synergistic effect to improve the biosensing performance.

Despite the obvious performance improvement by using the CP nanocomposite, such types of materials are still facing many challenges in practical sensing applications:

(1) Weak binding force between CPs and doping materials. Since the doping materials are always inorganic materials, the molecular force between CPs and inorganic materials is difficult to establish. Furthermore, it will cause the loss of adherence of the nanoparticles and performance degradation, especially in the case of usage over long periods. Therefore, the means to closely combine CPs and dopant materials to achieve performance optimization is an urgent problem.

(2) Poor anti-contamination ability of nanocomposites. Generally, in the actual detection system, whether it is blood, water, fermentation broth and other application systems, the environment is very complicated. In the actual detecting process, CPs have low anti-contamination ability and are easy to adhere to contaminants. Meanwhile, the active sites on the surface of CPs will be covered, which will adversely affect the detection performance. Hence, the targeted modification of CPs and increased anti-interference is one of the directions of future research.

(3) Swelling phenomenon of CPs resulting in poor stability. CPs often swells in solution, and the detection environment is mainly in aqueous electrolyte. In this case, the swelling phenomenon will accelerate removal of particles and affect the stability of the biosensor. Thus, how to select appropriate CP and doping materials to minimize the swelling effect is an important issue that needs attention in actual operation.

At present, there have been already much research on CPs nanocomposites based biosensors. However, realization of their transformation in practical applications is rarely reported. In order to address above issue, novel preparation methods are eagerly investigated, which are of high controllability and large-scale possibility to easily reproduce the nanostructure and properties of the composite. Besides, the influence of the swelling behaviour relevant to CPs and their biosensing performance requires discussion, which has generally existed but lacks attention. Online and dynamic detection is always a big challenge in all fields of clinical diagnosis, environmental monitoring fermentation process control, *etc.* Therefore, the surface characteristics of the nanocomposite film can be fine-tuned according to the main pollutants in different detection environments, providing satisfactory stability and potential for online testing. We believe that due to the advanced performance of CPs nanocomposites with regular morphologies, especially their excellent electrochemical stability, constructed biosensors have remarkable potential in product transformation for the analytical devices and associated instrumentation.

Conflicts of interest

There are no conflicts to declare.

Acknowledgements

This work was financially supported by the National Key R&D Program of China (No. 2021YFC2103300), the Joint Scientific Research Project of Sino Foreign Cooperative Education Platform in Jiangsu Universities Funded by Jiangsu Provincial Government, the National Natural Science Foundation of China (No. 22078148), the Natural Science Foundation of Jiangsu Province (No. BK20210549), the Natural Science Foundation of the Jiangsu Higher Education Institutions of China (No. 21KJB530007).

Notes and references

1 H. Teymourian, C. Moonla, F. Tehrani, E. Vargas, R. Aghavali, A. Barfidokht, T. Tangkuaram, P. P. Mercier, E. Dassau and J. Wang, *Anal. Chem.*, 2020, **92**, 2291–2300.

2 R. M. Cardoso, P. R. L. Silva, A. P. Lima, D. P. Rocha, T. C. Oliveira, T. M. Do Prado, E. L. Fava, O. Fatibello-Filho, E. M. Richter and R. A. A. Muñoz, *Sens. Actuators, B*, 2020, **307**, 127621.

3 S. H. Baek, J. Roh, C. Y. Park, M. W. Kim, R. Shi, S. K. Kailasa and T. J. Park, *Mater. Sci. Eng., C*, 2020, **107**, 110273.
4 C. Tseng, F. Liu, X. Zhang, P. Huang, I. Campbell, Y. Li, J. T. Atkinson, T. Terlier, C. M. Ajo-Frankin, J. J. Silberg and R. Verduzco, *Adv. Mater.*, 2022, **34**, 2109442.
5 B. M. Everett, M. M. Brooks, H. E. A. Vlachos, B. R. Chaitman, R. L. Frye and D. L. Bhatt, *N. Engl. J. Med.*, 2015, **373**, 610–620.
6 Z. Song, J. Song, F. Gao, X. Chen, Q. Wang, Y. Zhao, X. Huang, C. Yang and Q. Wang, *Sens. Actuators, B*, 2022, **368**, 132205.
7 A. Pourali, M. R. Rashidi, J. Barar, G. Pavon-Djavid and Y. Omidi, *Anal. Chem.*, 2021, **134**, 116123.
8 M. D. Gholami, A. P. O'Mullane, P. Sonar, G. A. Ayoko and E. L. Izake, *Anal. Chim. Acta*, 2021, **1185**, 339082.
9 S. Zhao, N. Liu, W. Wang, Z. Xu, Y. Wu and X. Luo, *Biosens. Bioelectron.*, 2021, **190**, 113466.
10 V. V. Tran, N. H. T. Tran, H. S. Hwang and M. Chang, *Biosens. Bioelectron.*, 2021, **182**, 113192.
11 S. Liu, Y. Ma, M. Cui and X. Luo, *Sens. Actuators, B*, 2018, **255**, 2568–2574.
12 Y. Chen, P. Yuan, A. Wanga, X. Luo, Y. Xue, L. Zhanga and J. Fenga, *Biosens. Bioelectron.*, 2019, **126**, 187–192.
13 X. Jiang, H. Wang, Y. Shen, N. Hu and W. Shi, *Sens. Actuators, B*, 2022, **350**, 130891.
14 S. Song, J. U. Lee, M. J. Jeon, S. Kim and S. J. Sim, *Biosens. Bioelectron.*, 2021, **199**, 1–10.
15 A. G. Ayankojo, R. Borozˇnjak, J. Reut, A. Opik and V. Syritski, *Sens. Actuators, B*, 2022, **353**, 131160.
16 E. D. Nascimento, W. T. Fonseca, T. R. de Oliveira, C. R. S. T. B. de Correia, V. M. Faça, B. P. de Morais, V. C. Silvestrini, H. Pott-Junior, F. R. Teixeira and R. C. Faria, *Sens. Actuators, B*, 2022, **353**, 131128.
17 G. Mao, Y. Li, G. Wu, S. Ye, S. Cao, W. Zhao, J. Lu, J. Dai and Y. Ma, *Sens. Actuators, B*, 2022, **369**, 132306.
18 L. C. Clark and C. Lyons, *Ann. N. Y. Acad. Sci.*, 1962, **102**, 29–45.
19 T. Chaibun, J. Puenpa, T. Ngamdee, N. Boonapatcharoen, P. Athamanolap, A. P. O'Mullane, S. Vongpunsawad, Y. Poovorawan, S. Y. Lee and B. Lertanantawong, *Nat. Commun.*, 2021, **12**, 802.
20 I. M. Mostafa, Y. Tian, S. Anjum, S. Hanif, M. Hosseini, B. Lou and G. Xu, *Sens. Actuators, B*, 2022, **365**, 131944.
21 E. Sehit and Z. Altintas, *Biosens. Bioelectron.*, 2020, **159**, 112165.
22 M. Holzinger, P. H. M. Buzzetti and S. Cosnier, *Sens. Actuators, B*, 2021, **348**, 130700.
23 X. Liu, W. Wu, D. Cui, X. Chen and W. Li, *Adv. Mater.*, 2021, **33**, 2004734.
24 F. Nasrin, I. M. Khoris, A. D. Chowdhury, J. Boonyakida and E. Y. Park, *Sens. Actuators, B*, 2022, **369**, 132390.
25 F. G. Zamani, H. Moulahoum, M. Ak, D. O. Demirkol and S. Timur, *Anal. Chem.*, 2019, **118**, 264–274.
26 C. K. Chiang, M. A. Druy, S. C. Gau, A. J. Heeger, E. J. Louis, A. G. MacDiarmid, Y. W. Park and H. Shirakawa, *J. Am. Chem. Soc.*, 1978, **100**, 1013–1035.
27 H. Shirakawa, T. Ito and S. Ikeda, *Macromol. Chem.*, 1978, **179**, 1565–1573.
28 R. Holze and Y. P. Wu, *Electrochim. Acta*, 2014, **122**, 93–107.
29 N. Aydemir, J. Malmstrom and J. Travas-Sejdic, *Phys. Chem. Chem. Phys.*, 2016, **18**, 8264–8277.
30 H. Tang, Y. Liang, C. Liu, Z. Hu, Y. Deng, H. Guo, Z. Yu, A. Song, H. Zhao, D. Zhao, Y. Zhang, X. Guo, J. Pei, Y. Ma, Y. Cao and F. Hua, *Nature*, 2022, **611**, 271–277.
31 S. Nie, Z. Li, Z. Su, Y. Jin, H. Song, H. Zheng, J. Song, L. Hu, X. Yin, Z. Xu, Y. Yao, H. Wang and Z. Li, *ChemSusChem*, 2023, **16**, e202202208.
32 B. Zhu, D. T. Bryant, A. Akbarinejad, J. Travas-Sejdic and L. I. Pilkington, *Polym. Chem.*, 2022, **13**, 508–516.
33 Z. Chen, E. Villani and S. Inagi, *Curr. Opin. Electrochem.*, 2021, **28**, 100702.
34 A. M. R. Ramírez, M. A. Gacitúa, E. Ortega, F. R. Díaz and M. A. Del Valle, *Electrochem. Commun.*, 2019, **102**, 94–98.
35 F. Fang, C. Liu, J. Zhong, Z. Zhan and Z. Huang, *Sens. Actuators, B*, 2022, **362**, 131759.
36 I. Y. Choi, J. Lee, H. Ahn, J. Lee, H. C. Choi and M. J. Park, *Angew. Chem., Int. Ed.*, 2015, **54**, 10497–10501.
37 F. Yin, D. Wang, Z. Zhang, C. Zhang and Y. Zhang, *Mater. Lett.*, 2017, **207**, 225–229.
38 L. Yang, Z. Zhang, G. Nie, C. Wang and X. Lu, *J. Mater. Chem. A*, 2015, **3**, 83–86.
39 T. Sun, J. Wang, N. A. Khoso, L. Yu and Y. Zhang, *Mater. Lett.*, 2017, **191**, 61–64.
40 A. McCarthy, J. V. John, L. Saldana, H. Wang, M. Lagerstrom, S. Chen, Y. Su, M. Kuss, B. Duan, M. A. Carlson and J. Xie, *Adv. Healthcare Mater.*, 2021, **10**, 2100766.
41 C. Bavatharani, E. Muthusankar, S. M. Wabaidur, Z. A. Alothman, K. M. Alsheetan, M. M. AL-Anazy and D. Ragupathy, *Synth. Met.*, 2021, **271**, 116609.
42 Y. Wang, A. Liu, Y. Han and T. Li, *Polym. Int.*, 2020, **69**, 7–17.
43 Z. Li, B. Li, B. Chen, J. Zhang and Y. Li, *Nanotechnology*, 2021, **32**, 395–503.
44 M. Lin, X. Hu, Z. Ma and L. Chen, *Anal. Chim. Acta*, 2012, **746**, 63–69.
45 A. Pruna, Q. Shao, M. Kamruzzaman, Y. Y. Li, J. A. Zapien, D. Pullini, D. B. Mataix and A. Ruotolo, *Appl. Surf. Sci.*, 2017, **392**, 801–809.
46 C. He, C. Yang and Y. Li, *Synth. Met.*, 2003, **139**, 539–545.
47 S. Kumar, P. Rai, J. G. Sharma, A. Sharma and B. D. Malhotra, *Adv. Mater. Technol.*, 2016, **1**, 1600056.
48 J. Muñoz and M. Pumera, *TrAC, Trends Anal. Chem.*, 2020, **128**, 115933.
49 H. Yuk, B. Lu, S. Lin, K. Qu, J. Xu, J. Luo and X. Zhao, *Nat. Commun.*, 2020, **11**, 1604.
50 F. Wei, T. Zhang, R. Dong, Y. Wu, W. Li, J. Fu, C. Jing, J. Cheng, X. Feng and S. Liu, *Nat. Protoc.*, 2023, **18**, 2459–2484.
51 N. C. Foulds and C. R. Lowe, *J. Chem. Soc., Faraday Trans. 1*, 1986, **82**, 1259–1264.
52 J. G. Ayenimo and S. B. Adeloju, *Talanta*, 2016, **148**, 502–510.

53 D. Maity and R. T. R. Kumar, *Biosens. Bioelectron.*, 2019, **130**, 307–314.
54 L. He, B. Cui, J. Liu, Y. Song, M. Wang, D. Peng and Z. Zhang, *Sens. Actuators, B*, 2018, **258**, 813–821.
55 H. Wang, H. Lü, L. Yang, Z. Song and N. Hui, *Anal. Chim. Acta*, 2020, **1139**, 155–163.
56 Z. Yu, H. Li, X. Zhang, N. Liu, W. Tan, X. Zhang and L. Zhang, *Biosens. Bioelectron.*, 2016, **75**, 161–165.
57 M. Şenel, I. Bozgeyik, E. Çevik and M. F. Abasıyanık, *Synth. Met.*, 2011, **161**, 440–444.
58 D. Jiang, Z. Chu, J. Peng and W. Jin, *Sens. Actuators, B*, 2016, **228**, 679–687.
59 Z. Chu, Y. Liu and W. Jin, *Biosens. Bioelectron.*, 2017, **96**, 17–25.
60 K. J. Stine, *Appl. Sci.*, 2019, **9**, 797.
61 Y. Xie, T. Liu, Z. Chu and W. Jin, *J. Electroanal. Chem.*, 2021, **893**, 1–17.
62 T. Zhang, R. Yuan, Y. Chai, W. Li and S. Ling, *Sensors*, 2008, **8**, 5141–5152.
63 K. Ghanbari and N. Hajheidari, *J. Polym. Res.*, 2015, **22**, 1–9.
64 M. R. A. Ramírez, M. A. Del Valle, F. Armijo, F. R. Díaz, M. Angélica Pardo and E. Ortega, *J. Appl. Polym. Sci.*, 2017, **134**, 44723.
65 W. Wang, W. Li, R. Zhang and J. Wang, *Synth. Met.*, 2010, **160**, 2255–2259.
66 F. Jiang, R. Yue, Y. Du, J. Xu and P. Yang, *Biosens. Bioelectron.*, 2013, **44**, 127–131.
67 X. Xiao, M. Wang, H. Li and P. Si, *Talanta*, 2013, **116**, 1054–1059.
68 B. M. Hryniewicz, J. Volpe, L. Bach-Toledo, K. C. Kurpel, A. E. Deller, A. L. Soares, J. M. Nardin, L. F. Marchesi, F. F. Simas, C. C. Oliveira, L. Huergo, D. E. P. Souto and M. Vidotti, *Mater. Today Chem.*, 2022, **24**, 100817.
69 J. Zhu, X. Liu, X. Wang, X. Huo and R. Yan, *Sens. Actuators, B*, 2015, **221**, 450–457.
70 X. Yang, L. Chi, C. Chen, X. Cui and Q. Wang, *Phys. E*, 2015, **66**, 120–124.
71 F. Meng, W. Shi, Y. Sun, X. Zhu, G. Wu, C. Ruan, X. Liu and D. Ge, *Biosens. Bioelectron.*, 2013, **42**, 141–147.
72 Z. Yang, C. Zhang, J. Zhang and W. Bai, *Biosens. Bioelectron.*, 2014, **51**, 268–273.
73 Y. Mai, X. Xia and X. Jie, *Mater. Res. Bull.*, 2017, **94**, 216–221.
74 Özge Lalegül-Ülker and Y. M. Elçin, *Mater. Sci. Eng., C*, 2021, **119**, 111600.
75 J. Xu, P. Yao, L. Liu, Z. Jiang, F. He, M. Li and J. Zou, *J. Appl. Polym. Sci.*, 2010, **118**, 2582–2591.
76 H. An, R. Zhang, Z. Li, L. Zhou, M. Shao and M. Wei, *J. Mater. Chem. A*, 2016, **4**, 18008–18014.
77 K. Qi, R. Hou, S. Zaman, B. Y. Xia and H. Duan, *J. Mater. Chem. A*, 2018, **6**, 3913–3918.
78 A. U. Haq, J. Lim, J. M. Yun, W. J. Lee, T. H. Han and S. O. Kim, *Small*, 2013, **9**, 3829–3833.
79 Z. Zhou and X. Wu, *J. Power Sources*, 2014, **262**, 44–49.
80 N. Song, W. Wang, Y. Wu, D. Xiao and Y. Zhao, *J. Phys. Chem. Solids*, 2018, **115**, 148–155.
81 Y. Sun, D. Liu, W. Liu, H. Liu, J. Zhao, P. Chen, Q. Wang, X. Wang and Y. Zou, *J. Phys. Chem. Solids*, 2021, **157**, 110235.
82 K. Itaya, I. Uchida and S. Toshima, *J. Phys. Chem.*, 1983, **87**, 105–112.
83 Z. Chu, L. Shi, Y. Liu, W. Jin and N. Xu, *Biosens. Bioelectron.*, 2013, **47**, 329–334.
84 Y. Xu, Z. Chu, L. Shi, J. Peng and W. Jin, *Sens. Actuators, B*, 2015, **221**, 1009–1016.
85 P. Yang, J. Peng, Z. Chu, D. Jiang and W. Jin, *Biosens. Bioelectron.*, 2017, **92**, 709–717.
86 P. Yang, J. Pang, F. Hu, J. Peng, D. Jiang, Z. Chu and W. Jin, *Sens. Actuators, B*, 2018, **276**, 31–41.
87 D. Jiang, J. Pang, Q. You, T. Liu, Z. Chu and W. Jin, *Biosens. Bioelectron.*, 2019, **124**, 260–267.
88 J. Feng, Y. Liu, M. Yang, C. Wu, W. Zhang, Z. Chu and W. Jin, *J. Electroanal. Chem.*, 2021, **900**, 115718.
89 T. Liu, Y. Xie, L. Shi, Y. Liu, Z. Chu and W. Jin, *Chin. J. Chem. Eng.*, 2021, **37**, 105–113.
90 S. Zhang, Y. Xie, J. Feng, Z. Chu and W. Jin, *AIChE J.*, 2021, **67**, e17142.
91 L. Li, J. Peng, Z. Chu, D. Jiang and W. Jin, *Electrochim. Acta*, 2016, **217**, 210–217.
92 S. Muthusamy, J. Charles, B. Renganathan and D. Sastikumar, *J. Mater. Sci.*, 2018, **53**, 15401–15417.
93 Z. Chu, W. Zhang, Q. You, X. Yao, T. Liu, G. Liu, G. Zhang, X. Gu, Z. Ma and W. Jin, *Angew. Chem., Int. Ed.*, 2020, **59**, 18701–18708.
94 G.-G. Lee and H.-G. Hong, *Electrochim. Acta*, 2023, **465**, 142949.
95 T. Uemura, M. Ohba and S. Kitagawa, *Inorg. Chem.*, 2004, **43**, 7339–7345.
96 T. Uemura, Y. Kadowaki, N. Yanai and S. Kitagawa, *Chem. Mater.*, 2009, **21**, 4096–4098.
97 T. Wang, M. Farajollahi, S. Henke, T. Zhu, S. R. Bajpe, S. Sun, J. S. Barnard, J. S. Lee, J. D. W. Madden, A. K. Cheetham and S. K. Smoukov, *Mater. Horiz.*, 2017, **4**, 64–71.
98 Y. Xie, X. Tu, X. Ma, M. Xiao, G. Liu, F. Qu, R. Dai, L. Lu and W. Wang, *Electrochim. Acta*, 2019, **311**, 114–122.
99 P. A. Palod and V. Singh, *Mater. Sci. Eng., C*, 2015, **55**, 420–430.
100 P. Jakhar, M. Shukla and V. Singh, *J. Mater. Sci.: Mater. Electron.*, 2019, **30**, 3563–3573.
101 Y. Xie and Y. Zhao, *Mater. Sci. Eng., C*, 2013, **33**, 5028–5035.
102 S. Komathi, A. I. Gopalan, N. Muthuchamy and K. P. Lee, *RSC Adv.*, 2017, **7**, 15342–15351.
103 C. Xiang, Y. Zou, S. Qiu, L. Sun, F. Xu and H. Zhou, *Talanta*, 2013, **110**, 96–100.
104 X. Chen, Z. Chen, R. Tian, W. Yan and C. Yao, *Anal. Chim. Acta*, 2012, **723**, 94–100.
105 Y. Aleeva, G. Maira, M. Scopelliti, V. Vinciguerra, G. Scandurra, G. Cannata, G. Giusi, C. Ciofi, V. Figa, L. G. Occhipinti and B. Pignataro, *IEEE Sens. J.*, 2018, **18**, 4869–4878.
106 C. Hou, D. Zhao, Y. Wang, S. Zhang and S. Li, *J. Electroanal. Chem.*, 2018, **822**, 50–56.

107 H. Al-Sagur, S. Komathi, H. Karakaş, D. Atilla, A. G. Gürek, T. Basova, N. Farmilo and A. K. Hassan, *Biosens. Bioelectron.*, 2018, **102**, 637–645.
108 M. A. Zahed, S. C. Barman, P. S. Das, M. Sharifuzzaman, H. S. Yoon, S. H. Yoon and J. Y. Park, *Biosens. Bioelectron.*, 2020, **160**, 112220.
109 M. Alagappan, S. Immanuel, R. Sivasubramanian and A. Kandaswamy, *Arabian J. Chem.*, 2020, **13**, 2001–2010.
110 T. L. Tran, T. X. Chu, D. C. Huynh, D. T. Pham, T. H. T. Luu and A. T. Mai, *Appl. Surf. Sci.*, 2014, **314**, 260–265.
111 E. Spain, T. E. Keyes and R. J. Forster, *Electrochim. Acta*, 2014, **109**, 102–109.
112 I. Tiwari, M. Gupta, C. M. Pandey and V. Mishra, *Dalton Trans.*, 2015, **44**, 15557–15566.
113 A. D. Chowdhury, R. Gangopadhyay and A. De, *Sens. Actuators, B*, 2014, **190**, 348–356.
114 J. Wilson, S. Radhakrishnan, C. Sumathi and V. Dharuman, *Sens. Actuators, B*, 2021, **171**, 216–222.
115 N. Hui, X. Sun, S. Niu and X. Luo, *ACS Appl. Mater. Interfaces*, 2017, **9**, 2914–2923.
116 T. Yang, L. Meng, J. Zhao, X. Wang and K. Jiao, *ACS Appl. Mater. Interfaces*, 2014, **6**, 19050–19056.
117 Y. Gu and M. Lai, *Biosens. Bioelectron.*, 2021, **31**, 124–129.
118 S. Radhakrishnan, C. Sumathi, A. Umar, S. J. Kim, J. Wilson and V. Dharuman, *Biosens. Bioelectron.*, 2013, **47**, 133–140.
119 K. Dağcı Kıranşan and E. Topçu, *ACS Appl. Nano Mater.*, 2020, **3**, 5449–5462.
120 Y. Duan, N. Wang, Z. Huang, H. Dai, L. Xu, S. Sun, H. Ma and M. Lin, *Mater. Sci. Eng., C*, 2020, **108**, 1–7.
121 P. Wang, L. Wang, M. Ding, M. Pei and W. Guo, *Analyst*, 2019, **144**, 5866–5874.
122 J. Moon, Y. H. Kim and Y. Cho, *Biosens. Bioelectron.*, 2014, **57**, 157–161.
123 P. Wang, F. Pei, E. Ma, Q. Yang, H. Yu, J. Liu, Y. Li, Q. Liu, Y. Dong and H. Zhu, *Bioelectrochemistry*, 2020, **131**, 1–8.
124 Y. Li, M. S. Khan, L. Tian, L. Liu, L. Hu, D. Fan, W. Cao and Q. Wei, *Anal. Bioanal. Chem.*, 2017, **409**, 3245–3251.
125 D. Song, J. Zheng, N. V. Myung, J. Xu and M. Zhang, *Talanta*, 2021, **225**, 1–11.
126 C. Zhao, C. Ma, M. Wu, W. Li, Y. Song, C. Hong and X. Qiao, *New J. Chem.*, 2020, **44**, 3524–3532.
127 A. Garcia-Cruz, F. Nessark, M. Lee, N. Zine, M. Sigaud, R. Pruna, M. Lopez, P. Marote, J. Bausells, N. Jaffrezic-Renault and A. Errachid, *Sens. Actuators, B*, 2018, **255**, 2520–2530.
128 F. Pei, P. Wang, E. Ma, Q. Yang, H. Yu, J. Liu, H. Yin, Y. Li, Q. Liu and Y. Dong, *J. Electroanal. Chem.*, 2019, **835**, 197–204.
129 J. Yukird, T. Wongtangprasert, R. Rangkupan, O. Chailapakul, T. Pisitkun and N. Rodthongkum, *Biosens. Bioelectron.*, 2017, **87**, 249–255.
130 G. Wang, A. Morrin, M. Li, N. Liu and X. Luo, *J. Mater. Chem. B*, 2018, **6**, 4173–4419.